8546 *J. Phys. Chem. A* **2000,** *104,* 8546−8550

Density-Functional Theory and Car-Parinello Study of Electronic, Structural, and Dynamical Properties of the Hexapyrrole Molecule

Renato Colle*,† and Alessandro Curioni‡

Scuola Normale Superiore, Piazza Dei Cavalieri, 56100 Pisa, Italy

Received: February 18, 2000

Electronic and structural properties of the ground state of the neutral and singly ionized hexapyrrole molecule are studied using density functional theory implemented with plane waves and pseudopotentials to include the effects of the core electrons. The calculated properties are compared with those of an infinite pyrrole chain in a regular 3D lattice of polypyrroles. The dynamical evolution of a charged defect along the chain of an isolated hexapyrrole created with a structural defect on a terminal ring is simulated using Car−Parrinello molecular dynamics. Information is obtained on coherence, time scale, and general features of the motion of the charge along the chain.

I. Introduction

The aim of this paper is, first, to compare the electronic and structural properties of an isolated, finite chain of pyrrole rings with those of the corresponding infinite chain in a regular 3D lattice of polypyrroles, thus identifying the differences that can be attributed mainly to environment effects. Second, using Car−Parrinello (CP) molecular dynamics,[1] we shall study the time evolution of a charged defect along the chain of an isolated hexapyrrole created with a structural defect on a terminal ring. The aim is to obtain information on coherence, time scale, and general features of the motion of a charge suddenly produced inside the distorted chain of a conjugated heterocycle polymer.

In a previous paper,[2] hereafter referred to as I, we have performed a density functional theory (DFT) study of neutral and doped polypyrroles, each of which is represented as a 3D lattice of infinite chains of pyrrole rings defined in terms of a fixed unit cell with internal degrees of freedom. The polypyrrole has been chosen as a prototype of the organic conjugated polymers that become conducting when properly doped and, thus, have attracted much interest both from a theoretical and an experimental point of view.[3,4,5] It is well-known from several sets of data that real polypyrroles are materials with low degrees of crystallinity, being mixtures of chains with large weight dispersion and different morphology. The presence of several chemical and structural defects makes it difficult to understand whether a property is intrinsically associated with the polymer or caused by defects. For these reasons, a crystalline lattice of infinite regular chains represents a model that contains only some of the peculiar features of the real systems and should be complemented by studying the properties of isolated pyrrole oligomers.

Moreover, regular ($\alpha - \alpha'$)-trans-dipyrrole oligomers, with up to seven pyrrole rings, have recently been synthesized and unambiguously characterized.[6] These compounds represent ideal systems for a theoretical study based on ab initio methods because their properties are intrinsically associated with those of an isolated chain and are affected only slightly by the environment.

In this paper, we investigate electronic, structural, and dynamical properties of an isolated hexapyrrole both neutral and singly ionized, and perform CP molecular dynamics in order to simulate transport phenomena inside a small chain and obtain information useful for polymers. We have chosen this oligomer because its structure is large enough to exhibit a conformational behavior resembling that of a typical polypyrrole chain, and the electronic properties are sufficiently similar to those of the polymer, as shown by our test calculations.[7,8]

II. Computational Procedures

All of the calculations presented in this paper have been performed with a code[9] that implements Kohn−Sham (KS) equations[10] and the CP method, using a basis set of plane waves (PW) together with a specific type of atomic pseudo-potentials.

As in I, we have used the DFT in the framework of the local spin density (LSD) approximation with the Becke and Perdew gradient corrections[11,12] for the exchange and the correlation energy, respectively. The Vanderbilt ultrasoft-pseudo-potentials[13] have been used for all of the atoms of the system, imposing an energy cutoff of 30 Ry in the PW expansion. Other computational details can be found in I.

To perform calculations of the isolated hexamer that are as similar as possible to those performed in I for a lattice of infinite regular chains of pyrrole rings, we have set up a periodic structure characterized by a big orthorhombic unit cell ($a = 52$ au, $b = 20.8$ au, $c = 20.8$ au) that contains the hexamer and used Hockney's method[14] to remove the effects due to the periodic boundary conditions.

As in complex systems, the identification of the minimum energy configuration is quite difficult, owing to the presence of several different local minima in the energy surface. We have performed each structural optimization in two steps: the first one used a "simulated annealing" procedure[15] to determine the region where the absolute minimum is located, and the second used a conjugate gradient to better refine the final values of the structural parameters.

---

* Scuola Normale Superiore, 56126 Pisa, Italy.

† Dipartimento di Chimica Applicata, Universitá di Bologna, Viale Risorgimento 2, 40136 Bologna, Italy,

‡ IBM Research Division, Zurich Research Laboratory, CH-8803 Rüschlikon, Switzerland..

10.1021/jp000661i CCC: $19.00

TABLE 1: Bond Distances (Å), Bond Angles, and Dihedral Angles (degrees) of the Hexapyrrole Molecule: Planar Conformation versus Out-of-Plane Conformation (in Parentheses)

N_1-C_1	1.393 (1.395)	N_3-C_9	1.400 (1.400)	N_5-C_{17}	1.399 (1.400)
N_1-C_4	1.399 (1.385)	N_3-C_{12}	1.399 (1.401)	N_5-C_{20}	1.399 (1.398)
C_1-C_2	1.384 (1.382)	C_9-C_{10}	1.400 (1.400)	$C_{17}-C_{18}$	1.399 (1.396)
C_2-C_3	1.425 (1.433)	$C_{10}-C_{11}$	1.418 (1.420)	$C_{18}-C_{19}$	1.419 (1.425)
C_3-C_4	1.398 (1.400)	$C_{11}-C_{12}$	1.400 (1.400)	$C_{19}-C_{20}$	1.398 (1.398)
C_4-C_8	1.447 (1.458)	N_3-H_8	1.025 (1.025)	N_5-H_{14}	1.025 (1.026)
N_1-H_1	1.025 (1.027)	$C_{10}-H_9$	1.092 (1.092)	$C_{18}-H_{15}$	1.092 (1.090)
C_1-H_2	1.090 (1.088)	$C_{11}-H_{10}$	1.092 (1.091)	$C_{19}-H_{16}$	1.092 (1.091)
C_2-H_3	1.090 (1.090)	$C_{12}-C_{16}$	1.443 (1.446)	$C_{20}-C_{24}$	1.447 (1.449)
C_3-H_4	1.093 (1.090)			N_6-C_{21}	1.393 (1.392)
N_2-C_5	1.399 (1.399)	N_4-C_{13}	1.400 (1.399)	N_6-C_{24}	1.399 (1.401)
N_2-C_8	1.399 (1.400)	N_4-C_{16}	1.399 (1.398)	$C_{21}-C_{22}$	1.384 (1.385)
C_5-C_6	1.399 (1.400)	$C_{13}-C_{14}$	1.400 (1.397)	$C_{22}-C_{23}$	1.425 (1.437)
C_6-C_7	1.419 (1.421)	$C_{14}-C_{15}$	1.418 (1.422)	$C_{23}-C_{24}$	1.398 (1.402)
C_7-C_8	1.398 (1.395)	$C_{15}-C_{16}$	1.400 (1.399)	N_6-H_{17}	1.025 (1.027)
C_5-C_9	1.444 (1.448)	$C_{13}-C_{17}$	1.444 (1.446)	$C_{21}-H_{18}$	1.090 (1.089)
N_2-H_5	1.025 (1.026)	N_4-H_{11}	1.025 (1.026)	$C_{22}-H_{19}$	1.090 (1.090)
C_6-H_6	1.092 (1.092)	$C_{14}-H_{12}$	1.092 (1.092)	$C_{23}-H_{20}$	1.093 (1.096)
C_7-H_7	1.092 (1.092)	$C_{15}-H_{13}$	1.092 (1.092)		
$C_3C_4C_8C_7$	0 (43.8)	$C_6C_5C_9C_{10}$	0 (3.2)	$C_{11}C_{12}C_{16}C_{15}$	0 (22.3)
$C_{14}C_{13}C_{17}C_{18}$	0 (31.2)	$C_{19}C_{20}C_{24}C_{23}$	0 (20.1)		

Figure 1. Optimized structure of neutral hexapyrrole.

III. Neutral and Singly Ionized Hexapyrroles

In this section, we investigate the electronic and structural properties of the ground state of an isolated hexapyrrole both neutral and singly ionized. First of all, we want to answer the questions about the planarity of an isolated pyrrole chain and the modifications induced by the oxidation of the system. Previous theoretical attempts to investigate these problems were limited to small oligomers, often studied using semiempirical methods that are known to give inaccurate torsional potentials around single bonds.[16] Moreover, until now, no experimental vapor phase information has been available because the experimental data, recently obtained for pyrrole oligomers with chains up to seven pyrrole rings, have been recorded in solutions of acetonitrile.[6] Therefore, the present ab initio calculations constitute the first realistic attempt to answer the previous questions.

The results of the calculations reported in I show that an infinite, neutral chain of pyrrole rings in a 3D periodic arrangement is planar, whereas deviations from the planarity are induced by doping agents. However, one can argue that these results are, at least in part, an artifact of the periodic boundary conditions characteristic of the computational procedure chosen. Therefore, we have set up a type of ab initio calculation for the isolated oligomer that is as similar as possible to that performed for the periodic system. Furthermore, we study the hexapyrrole because its structure is large enough to exhibit conformational behavior and electronic properties similar to those of the polymeric chains, as shown by our preliminary calculations[7,8] on a sequence of pyrrole oligomers with different chain lengths.

We have optimized the structures of the neutral and the singly ionized hexapyrrole both constraining the molecule to keep a planar ($\alpha - \alpha'$)-trans-conformation and removing this constraint to start from random out-of-plane conformations to determine the minimum energy conformation.

Let us consider first the neutral oligomer. We have found that the planar conformation is less stable than the out-of-plane one by about 15 kcal/mol. This result agrees well with the fact that small deviations from planarity do not drastically reduce the stabilization energy due to conjugation but simultaneously lower the steric repulsion between the in-plane groups. This interpretation is also confirmed by the comparison between KS eigenvalues of the in-plane and out-of-plane conformers, whose differences are, in general, small (less than 10%). Table 1 compares the structural parameters obtained for the in-plane and the out-of-plane conformation, the latter shown in Figure 1. Atoms of the same type are labeled clockwise on each pyrrole ring, as in I.

By comparing the two structures, we see that the planar conformation preserves the C_{2h} symmetry, whereas the out-of-plane conformation does not preserve the symmetry. The bond-length alternation in the carbon−carbon backbone decreases from the border to the center of the chain in both the structures, a fact that indicates larger conjugation in the central rings than in the terminal ones. To confirm this result, we have used, as in I, the F function that is defined for each pyrrole ring as follows: $F = d_1/d_2$, where d_1 is the length of the C2−C3 bond (formally a single bond in an isolated pyrrole), and d_2 is the average length of the C1−C2 and C3−C4 bonds (formally double bonds). This function gives a measurement of the relative importance of the “aromatic” character with respect to the “quinoid” character of the structure, where “quinoid” refers to a structure in which C2−C3 and the inter-ring bond C4−C8 have a greater double-bond character than in the standard (aromatic) configuration of an isolated dipyrrole. The analysis of this function, whose values are reported in Table 2, shows that, in both configurations, the center of the chain has a greater quinoid character than that of the terminal parts, where the π−conjugation ends. For the out-of-plane conformation, the increase of the torsional angles from the center toward the ends of the chain lowers the π-conjugation and yields greater values to the inter-ring bond lengths and, therefore, to the F function.

Let us now consider a singly ionized hexapyrrole. In this case, the out-of-plane conformation is only 1.5 kcal/mol more stable than the planar one. One may also observe that the four central rings lie approximately on the same plane, whereas the ending rings bend out of this plane, as shown in Figure 2 and confirmed by the structural parameters reported in Table 3.

The radical cation shows a quinoid structure localized in the central part of the chain, whereas the aromatic conjugation is preserved on the external rings. Thus, the only possible rotations

Figure 2. Optimized structure of singly ionized hexapyrrole.

TABLE 2: Values of F_n (Where n Indicates the Progressive Number of the Ring in the Chain) and of the Inter-rings Bond Lengths (Å) in the Neutral Hexamer: Planar (P) versus Out-of-Plane (OP) Conformation

	P	OP
F_1	1.024	1.036
R1−R2	1.447	1.458
F_2	1.015	1.017
R2−R3	1.444	1.448
F_3	1.013	1.014
R3−R4	1.443	1.446
F_4	1.013	1.017
R4−R5	1.444	1.446
F_5	1.015	1.020
R5−R6	1.447	1.449
F_6	1.024	1.033

are those around the final inter-ring C−C bonds, which maintain a single-bond character. This result is confirmed by inspection of the F function and of the inter-ring bond lengths reported in Table 4.

The structural modifications that are induced by the ionization process are well localized on the four central rings and very similar in the two conformers. The most relevant differences are localized on the terminal inter-ring bonds that, in the planar conformation, maintain a greater double-bond character than in the out-of-plane conformer. In Table 5, we list the values of the net charge on each pyrrole ring calculated with the Mulliken Population Analysis, and the excess spin density on each pyrrole ring. The analysis of these data suggests the following conclusions:

- The positive charge is localized mainly on the two ending rings, whereas the excess spin density is distributed primarily on the central rings of the chain.
- The two conformers have similar distributions of charge and excess spin density, with a small asymmetry in the out-of-plane conformer.

The structural parameters obtained from these calculations suggest that the modifications induced by a local oxidation of an infinite chain should involve more than six rings because, in the hexamer, the effects on the terminal rings are still relevant. A comparison between the structural data of the two systems indicates that the planar conformation is preferred by the infinite chains of the neutral polypyrrole but not by the neutral hexapyrrole molecule. This difference can be ascribed both to the larger extent of the conjugation in an infinite chain, a fact that increases the double-bond character of the inter-ring bonds, and to the presence of the neighboring chains in the 3D lattice, where the planar conformation minimizes the interchain repulsion.

On the other hand, although the oxidized polymers studied in I show a more or less pronounced out-of-plane deformation of the chains, increased further by the presence of doping agents, an oxidized hexapyrrole molecule assumes a conformation that is appreciably distorted from the planarity only in the terminal rings. This fact can be ascribed mainly to the strong interaction in the polymer between charged chains, and, in the case of doped polypyrroles, to the steric hindrance of the doping agent and its electronic interaction with the pyrrole chains.

IV. Motion of a Charged Defect along a Hexapyrrole Chain

In this section, we present the results of a molecular dynamics simulation of the intrachain charge transport along the chain of an isolated hexapyrrole. We shall study the motion of a charged defect suddenly produced inside a regular ($\alpha - \alpha'$)-trans-hexapyrrole in greater detail, using CP molecular dynamics. In this approach, the interatomic forces are computed from an electronic structure calculation based on the DFT and performed “on the fly,” i.e., during the dynamical process. The interatomic potential is parameter-free, derived from first principles with no experimental input and governs the nuclear motion according to the classical laws of motion. A central assumption of the method is the validity of the Born−Oppenheimer (BO) approximation. This means that the gap between the ground state and the first excited state of the electronic system is much greater than the energy associated with the ionic motion. If this condition is satisfied, the behavior of the coupled electron−ion system can be regarded as adiabatic, and the nuclear motion follows the BO energy surface.

The initial structure has been prepared by substituting one of the ending rings in the neutral hexapyrrole structure with a “quinoid” ring, taken from the optimized structure of a singly ionized trans-dipyrrole. In this way, we have prepared a localized defect near the end of the molecule, whose dynamical relaxation toward a stable structure of the chain is simulated using CP molecular dynamics.

We start with a planar chain of six pyrrole rings having the following sequence: Q, A, A, A, A, A (where A indicates aromatic and Q quinoid structure) and calculate the electronic wave function that corresponds to the ground state of the singly ionized system in the above configuration. The dynamical evolution of the charge distribution along the chain is followed by looking at the time evolution of the net charge on each pyrrole ring, calculated with the Mulliken Population Analysis, see Table 6, and by looking at the time evolution of the excess spin-density distribution, reported in Figures 3 and 4 for different time steps.

At the beginning of the simulation, as expected, the quinoid-like structure of the first ring favors a partial localization of the positive charge on this ring, whereas the excess spin density, which yields the probability distribution of the unpaired electron, is localized mainly on the other side of the chain where the structure is still aromatic, see Figure 3.

Starting from this configuration, we have followed the free dynamics of the relaxation process for a time period of 0.5 ps. This process can be subdivided into two parts:

- During the first time interval (about 100 fs), the charge distribution carries out a sequence of dumped oscillations: the positive charge runs back and forth from one end of the chain to the other with oscillations that are progressively damped.
- During the second time interval (about 400 fs), the charged hexamer stabilizes in its final conformation, and the charge distribution converges progressively to the distribution characteristic of the charged hexamer studied previously.

Figure 4 shows the spin-density distribution after 100 fs. We see that the unpaired electron is localized mainly on the left part of the chain (first three rings) after its “reflection” by the ending ring. Table 7 lists the values of the F function at different time steps to identify possible correlations between charge and structural relaxations. The following conclusions can be drawn:

- The time evolution of the structural deformation, see Table 7, is similar to that of the charge distribution, see Table 6. This fact confirms the existence of a direct relationship between

TABLE 3: Bond Distances (Å), Bond Angles, and Dihedral Angles (degrees) of a Charged (+1) Hexapyrrole Molecule: Planar Conformation versus Out-of-Plane Conformation (in Parentheses)

N_1-C_1	1.385 (1.388)	N_3-C_9	1.397 (1.397)	N_5-C_{17}	1.403 (1.401)
N_1-C_4	1.402 (1.404)	N_3-C_{12}	1.400 (1.400)	N_5-C_{20}	1.394 (1.395)
C_1-C_2	1.391 (1.386)	C_9-C_{10}	1.415 (1.413)	$C_{17}-C_{18}$	1.411 (1.408)
C_2-C_3	1.415 (1.420)	$C_{10}-C_{11}$	1.400 (1.404)	$C_{18}-C_{19}$	1.403 (1.402)
C_3-C_4	1.403 (1.408)	$C_{11}-C_{12}$	1.415 (1.420)	$C_{19}-C_{20}$	1.413 (1.409)
C_4-C_8	1.436 (1.442)	N_3-H_8	1.025 (1.025)	N_5-H_{14}	1.026 (1.029)
N_1-H_1	1.026 (1.024)	$C_{10}-H_9$	1.091 (1.091)	$C_{18}-H_{15}$	1.091 (1.092)
C_1-H_2	1.090 (1.088)	$C_{11}-H_{10}$	1.091 (1.090)	$C_{19}-H_{16}$	1.091 (1.091)
C_2-H_3	1.090 (1.091)	$C_{12}-C_{16}$	1.428 (1.424)	$C_{20}-C_{24}$	1.436 (1.441)
C_3-H_4	1.092 (1.090)			N_6-C_{21}	1.385 (1.386)
N_2-C_5	1.403 (1.399)	N_4-C_{13}	1.397 (1.399)	N_6-C_{24}	1.402(1.404)
N_2-C_8	1.394 (1.401)	N_4-C_{16}	1.400 (1.400)	$C_{21}-C_{22}$	1.391 (1.383)
C_5-C_6	1.411 (1.410)	$C_{13}-C_{14}$	1.415 (1.417)	$C_{22}-C_{23}$	1.415 (1.418)
C_6-C_7	1.403 (1.408)	$C_{14}-C_{15}$	1.400 (1.408)	$C_{23}-C_{24}$	1.403 (1.404)
C_7-C_8	1.413 (1.416)	$C_{15}-C_{16}$	1.415 (1.414)	N_6-H_{17}	1.026 (1.024)
C_5-C_9	1.429 (1.424)	$C_{13}-C_{17}$	1.429 (1.424)	$C_{21}-H_{18}$	1.090 (1.090)
N_2-H_5	1.026 (1.026)	N_4-H_{11}	1.025 (1.019)	$C_{22}-H_{19}$	1.090 (1.090)
C_6-H_6	1.091 (1.091)	$C_{14}-H_{12}$	1.091 (1.091)	$C_{23}-H_{20}$	1.092 (1.092)
C_7-H_7	1.091 (1.091)	$C_{15}-H_{13}$	1.091 (1.092)		
$C_3C_4C_8C_7$	0 (28.7)	$C_6C_5C_9C_{10}$	0 (1.8)	$C_{11}C_{12}C_{16}C_{15}$	0 (0.6)
$C_{14}C_{13}C_{17}C_{18}$	0 (7.9)	$C_{19}C_{20}C_{24}C_{23}$	0 (28.4)		

TABLE 4: Values of F_n (Where n Indicates the Progressive Number of the Ring in the Chain) and of the Inter-rings Bond Lengths (Å) in a Charged (+1) Hexamer: Planar (P) versus Out-of-Plane (OP) Conformation

	P	OP
F_1	1.013	1.016
R1−R2	1.436	1.442
F_2	0.994	0.996
R2−R3	1.429	1.424
F_3	0.989	0.995
R3−R4	1.428	1.424
F_4	0.989	0.995
R4−R5	1.429	1.424
F_5	0.994	0.996
R5−R6	1.436	1.441
F_6	1.013	1.017

TABLE 5: Charge and Excess Spin-density on Each Pyrrole Ring of the In-plane and Out-of-Plane (in Parentheses) Conformers. All Quantities Are in Atomic Units

ring	charge	spin density
1	0.31 (0.28)	−0.12 (−0.11)
2	0.04 (0.02)	−0.18 (−0.18)
3	0.15 (0.19)	−0.20 (−0.22)
4	0.15 (0.16)	−0.20 (−0.21)
5	0.04 (0.09)	−0.18 (−0.18)
6	0.31 (0.26)	−0.12 (−0.10)

TABLE 6: Net Charges on Each Pyrrole Ring and Their Increments (in Parentheses) from the Previous Values Given as Functions of Time. All Quantities Are in Atomic Units

time (fs)	0	50	100	150
ring 1	0.46	0.30 (−0.16)	0.27 (−0.03)	0.25 (−0.02)
ring 2	0.22	0.04 (−0.18)	0.10 (+0.06)	0.08 (−0.02)
ring 3	0.22	0.15 (−0.07)	0.15 (0.00)	0.18 (+0.03)
ring 4	0.05	0.17 (+0.12)	0.08 (−0.09)	0.14 (+0.06)
ring 5	−0.13	0.05 (+0.18)	0.15 (+0.10)	0.07 (−0.08)
ring 6	0.18	0.29 (+0.11)	0.25 (−0.04)	0.28 (+ 0.03)

charge localization and quinoid deformation. To elaborate, after about 50 fs the configuration QAAAAA changes into AQQQQA, with a corresponding big shift of the charges among the pyrrole rings. During the following time period, the activated vibrational mode, which changes alternatively aromatic into quinoid structure of each ring, loses its coherence and the charge oscillations are damped.

- The second part of the CP dynamics shows a stabilization of the quinoid deformation in the middle of the chain, whereas the two ending rings start assuming an out-of-plane conformation.

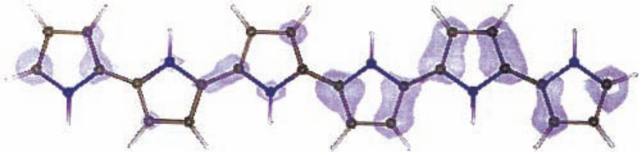

Figure 3. Excess of spin density distribution in the initial configuration: 0.0015 au isovalue surface.

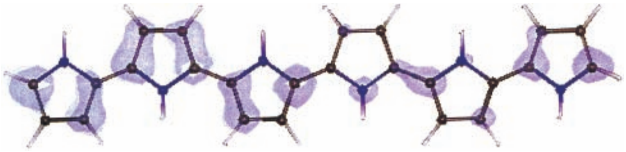

Figure 4. Excess of spin density distribution in the configuration after 100 fs; 0.0015 au isovalue surface.

TABLE 7: Values of the F Function on the Six Pyrrole Rings of the Chain Given as Functions of Time

time(fs)	0	50	100	150
F_1	0.984	1.017	1.013	1.011
F_2	1.016	0.994	0.996	0.994
F_3	1.016	0.989	0.980	0.980
F_4	1.016	0.990	0.979	0.983
F_5	1.016	0.990	0.980	0.983
F_6	1.016	1.007	1.012	1.010

Finally, we have studied the time evolution of the dihedral angles that define the torsion of the two ending rings with respect to the adjacent ones, see Figure 5.

This torsion is governed by the progressive breaking of the π-conjugation between ending rings and the rest of the chain, which forces the inter-ring bonds between central rings to maintain a double-bond character. As the quinoid deformation increases the double-bond character of the inter-ring bonds and, therefore, the barrier of the out-of-plane deformation, as long as this structure remains in the proximity of the ending rings, they are forced to stay coplanar with the other rings, whereas the localization of the quinoid structure on the central part of the chain frees the ending rings to get out of plane. In particular, we see from Figure 5 that, after 100 fs, when the quinoid deformation is localized on the right-hand side of the chain, the torsion around the first inter-ring bond starts to increase, whereas the other terminal ring starts about 100 fs later the same

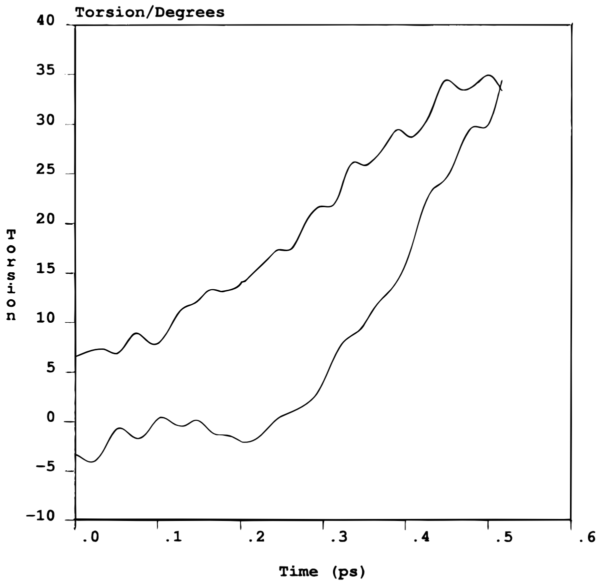

Figure 5. Time evolution of the torsional angles ($N_1-C_4-C_8-C_7$) between first and second rings (upper line) and ($N_6-C_{24}-C_{20}-C_{19}$) between fifth and sixth rings (lower line). Time is given in fs.

torsion around the inter-ring bond. At the end of the simulation, the two dihedral angles reach the same value (~35°), close to the value (~28°) characteristic of the minimum energy configuration, see Table 3.

V. Conclusions

We can summarize our results as follows:

- For the neutral hexapyrrole molecule, the out-of-plane conformation, although less conjugated and, therefore, more aromatic in character, is lower in energy by about 15 kcal/mol than the in-plane one. This result is in contrast with the almost perfect planarity of the infinite chains of the neutral polypyrrole in a 3D periodic arrangement, see I. This difference can be ascribed mainly to solid-state environment effects. The absence of neighboring chains, indeed, allows the stabilization of the hexapyrrole molecule also through small out-of-plane deformations, which reduce the steric repulsion between the in-plane groups without lowering the π-conjugation too much.
- For the singly ionized hexapyrrole molecule, the out-of-plane conformer is only 1.5 kcal/mol more stable than the in-plane one, a difference that is of the same order of magnitude as the uncertainty in the energy differences calculated with our method. Both conformers have a much greater quinoid character than the corresponding ones of the neutral hexapyrrole. The excess spin density is localized on the central rings and decreases progressively toward the terminal rings, where the positive charge is mainly localized. Compared with the best structure of the chains of an oxidized polypyrrole having one hole every four rings, see I, we see that the out-of-plane deformation in the polymer chains is much larger than that observed in the central part of the chain of an isolated hexapyrrole, where only the ending rings have appreciable values of the torsional angles.
- The CP molecular dynamics proves to be an important tool to follow the time evolution of local perturbations applied to complex systems and, thus, to study transport properties in real systems without introducing unrealistic models. Our calculations constitute a first step in this direction.

References and Notes

(1) Car, R.; Parrinello, M. *Phys. Rev. Lett.* **1985**, *55*, 247.

(2) Colle, R.; Curioni, A. *J. Am. Chem. Soc.* **1998**, *120*, 4832, and references therein.

(3) Skotheim, Terje, A., Ed. *Handbook of Conducting Polymers*; Marcel Dekker: New York, 1986, and references therein.

(4) Salaneck, W. R.; Clark, D. T.; Saumelsen, E. J. *Science and Application of Conducting Polymers*; Adam Hilger, Bristol, 1991.

(5) Salaneck, W. R.; Lundstron, I.; Ranby, B. *Conjugated Polymers and Related Materials: The Interconnection of Chemical and Electronic Structure*; Oxford University Press: London, 1993.

(6) Zotti, G.; Martina, S.; Wegner, G.; Schlüter, A.-D. *Adv. Mater.* **1992**, *4*, 798.

(7) Curioni, A. Ph.D. Thesis, Scuola Normale Superiore, Pisa, 1997.

(8) Colle, R.; Montagnani, R.; Salvetti, O. *Theor. Chem. Acc.* **1999**, *101*, 262.

(9) CPMD Version 2.5, Copyright (c) 1994 IBM Corporation.

(10) Kohn, W.; Sham, L. J. *Phys. Rev.* **1965**, *140*, A1133.

(11) Becke, A. D. *Phys. Rev. A* **1988**, *38*, 3098.

(12) Perdew, J. P. *Phys. Rev. B* **1986**, *33*, 882.

(13) Vanderbilt, D. *Phys. Rev. B* **1993**, *47*, 10 142.

(14) Barnett, R. N.; Landman, U. *Phys. Rev. B* **1993**, *48*, 2081.

(15) Kirchpatrick, S.; Gelatt, C. D.; Vecchi, M. P. *Science* **1983**, 220, 671.

(16) Kofranek, M.; Kovar, T.; Karpfen, A.; Lischka, H. *J. Chem. Phys.* **1992**, *94*, 4464.